A ROOT-based detector test system

Huang-Kai Wu[1,2] · Chen Li[1,3]

Abstract Most detectors for nuclear physics experiments are detector arrays composed of numerous units. Testing each detector unit is a major part of the research work on detector arrays. To save time and simplify the research process, a ROOT-based detector test system was designed for detector unit testing. The test system is a general purpose and expandable software system that can support most of the hardware devices in the market. Users can easily build a complete detector test system using the required hardware devices. The software is based on the ROOT framework and is operated on the Linux platform. The software of the test system consists of four parts: the controller, data acquisition(DAQ), high-voltage power supply, and online monitoring and analysis. In addition, a user-friendly graphical user interface (GUI) was designed for user convenience. Moreover, the online analysis function of the software can implement automatic peak searching and spectrum fitting for different radioactive sources, and the results under different conditions can be shown automatically. The completion of the test system could greatly simplify the development process of the detector.

Keywords Detector test · Data analysis · ROOT

✉ Chen Li
lichen@zjlab.org.cn

1   Shanghai Institute of Applied Physics, Chinese Academy of Sciences, Shanghai 201800, China

2   University of Chinese Academy of Sciences, Beijing 100049, China

3   Shanghai Synchrotron Radiation Facilitiy, Zhangjiang Laboratory, Shanghai Advanced Research Institute, Shanghai 201204, China

1 Introduction

Detectors in domestic and foreign laboratories are usually detector arrays, which are composed of many identical detector units. For example, the Advanced Gamma Tracking Array (AGATA) is the next generation γ-ray spectrometer of the European project, which is composed of 180 HPGe detector units, covering 4π solid angles [1].The ELI-NP GANT–Thermal Neutrons array (ELI-GANT-TN) is a 4π neutron detector consisting of 30 ^{3}He counters embedded in polyethylene, which is used for photo-neutron cross section measurements [2]. The ELI-NP Silicon Strip Array (ELISSA) consists of three rings of twelve single-sided X3 Si strip detectors, that are designed for photo-dissociation reactions relevant to Big Bang nucleosynthesis (BBN), supernova explosions, and p-process studies [3]. Other types of detector units include HPGe detector arrays [4–7], neutron detector arrays [8–11], silicon detector arrays [12–15], and the liquid scintillator dark matter detector [16–18]. Consequently, unit tests are an important process in the development of detector arrays. To obtain the best operating parameters, time-consuming and repeated unit tests are often required. During the development of the CsI detector array designed by the Shanghai Institute of Applied Physics encountered the same problem [19]. To overcome this problem, a ROOT-based detector test system was developed that can automatically adjust the working parameters of the detector and analyze the data.

Moreover, owing to the modular design of this test system, it can be easily expanded into a versatile test system to meet different test requirements.

ROOT, a common data analysis software package used in nuclear physics, has both a powerful data analysis function and a flexible graphical user interface(GUI) design function. ROOT has been widely used in many projects. Examples of such projects include the DAQ system for the silicon pixel detector, NDAQ system of the Heavy Ion Medical Machine (HIMM) of Lanzhou Institute of Modern Physics, and the General-Purpose Digital Data Acquisition System (GDDAQ)of Peking University [20–23]. Therefore, ROOT [24] is suitable for implementation of the detector test system. Along with the development of advanced hardware, many newer nuclear electronic modules support remote control. The maturity of hardware and software makes it possible to develop a test system that can simplify the test process of the detector unit.

Compared with the common DAQ system, our detector test system has the following characteristics. First, the test system can support more types of hardware devices than the DAQ system. The test system not only includes the DAQ function, but also the functions of controlling the main amplifier and high-voltage power-supply module. Second, for detector testing, the test system runs quickly, sometimes requiring only 10 min. After sufficient statistics are acquired, the DAQ loop can be completed. Third, to obtain the best parameters, the voltage and gain of the detector should be treated as variables under each test. Since the radioactive source is known, the analysis algorithm is universal. Therefore, the test system can integrate the data analysis function into the software. In contrast, common DAQ systems do not integrate data analysis functions in the software since different experiments have different experimental purposes.

The remainder of this paper is organized as follows: Sect. 2 presents the hardware architecture of the test system. Section 3 describes the software framework and GUI. Finally, the feasibility and stability of the system are tested in Sect. 4, and a summary is provided in Sect. 5.

2 Hardware support of test system

Detector test systems usually involve several functional modules, such as a high-voltage power supply module, preamplifier, main amplifier, and analog-to-digital conversion module(ADC, TDC, flash ADC, etc.). Depending on the type of interface, modules can be divided into three types: NIM, VME, and desktop modules. Therefore, the software of the test system needs to support these three types of hardware devices. Usually, the connection between a device and a PC is through a USB interface or an optical fiber link. As shown in Fig. 1, the hardware of the test system can be divided into four parts: the desktop module, NIM, VME, and a PC for control and data acquisition. The instruction communication between various hardware devices is implemented uniformly through the controller module of the software. Data can be obtained not only by modules with VME interfaces, but also by desktop modules, such as DT5720. The trigger signal can be provided externally via the front panel trigger input, as well as via the software. Alternatively, each channel can generate a self-trigger signal when the digitized input pulse exceeds a configurable threshold set through the register address. DT5720 houses USB 2.0, and the optical link interfaces. USB 2.0, allows data transfers up to 30 MB/s. The optical link supports a transfer rate of 80 MB/s and offers a daisy chain capability. This was successfully added to the test system. Normally, NIM devices can also be used for data acquisition. However, because of fewer functions and the existence of alternative products, NIM devices with DAQ functions were not considered for the test system design.

A CsI detector test system was built to verify the feasibility of the test system. The principal components of hardware for this system are the VME and NIM modules, as well as the desktop high voltage module with independent USB interfaces. The VME modules used were ADC(V785) and MADC-32 [25, 26]. In addition, the data acquisition module also includes DT5720 [27], which is linked to the PC via the USB interface. The NIM module includes the shaping amplifier MSCF-16 [27] and the gate and delay generator GG8020 manufactured by ORTEC. The VME controller selects the V2718 manufactured by CAEN and is connected to the PCI card using optical fibers. The maximum data transfer rate is 80MB byte/s. DT5533 is a desktop module housing four independent high voltage power supply channels with an independent USB interface, which can be controlled and monitored by software [28]. The specific test process is presented in Sec. 4.

3 Description of test system

The following software was developed to conveniently obtain and handle the raw data: the Controller module, HV_module, DAQ_module, and Online_module. Instruction communication and data transmission between different components are implemented through shared memory. The Controller_module is the main control part, which is used to send data acquisition instructions and feedback status parameters of hardware devices. The data
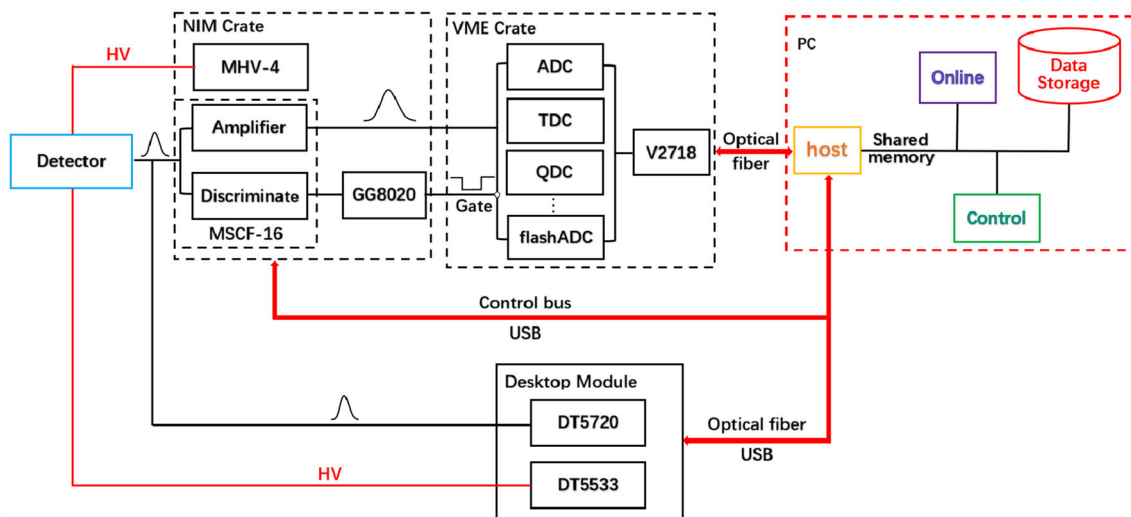
Fig. 1 System architecture

acquisition software, DAQ_module, is responsible for implementing data acquisition, transmission, and storage functions according to the received instructions. The HV_module is responsible for adding voltage to the detector according to the working parameters set by the Controller_module. The Online_module's monitoring and analysis components can implement the online data monitoring and analysis functions.

3.1 Framework of software

The relationships between the four parts are shown in Fig. 2. The Controller_module consists of two parts: DAQ_Control and HV_Control. DAQ_Control is responsible for sending data acquisition instructions and setting data acquisition parameters. The corresponding instructions are transmitted to the shared memory, received, and executed by the DAQ. HV_Control is responsible for setting the working parameters of high-voltage devices. Similarly, the parameters are written into the shared memory and read by HV_Control. After HV_Control receives the working parameters from the shared memory, the high-voltage module DT5533 is initialized with the setting value, and the corresponding voltage is applied to the detector. Each time HV_Control completes a voltage addition operation; it feeds back the status parameters to the Controller_module. The control function of the Controller_module is realized by calling the shared memory class and the control GUI class defined in the software. The parameter passed to the shared memory class is the defined structure, which includes the working parameters of the high-voltage devices, the data acquisition
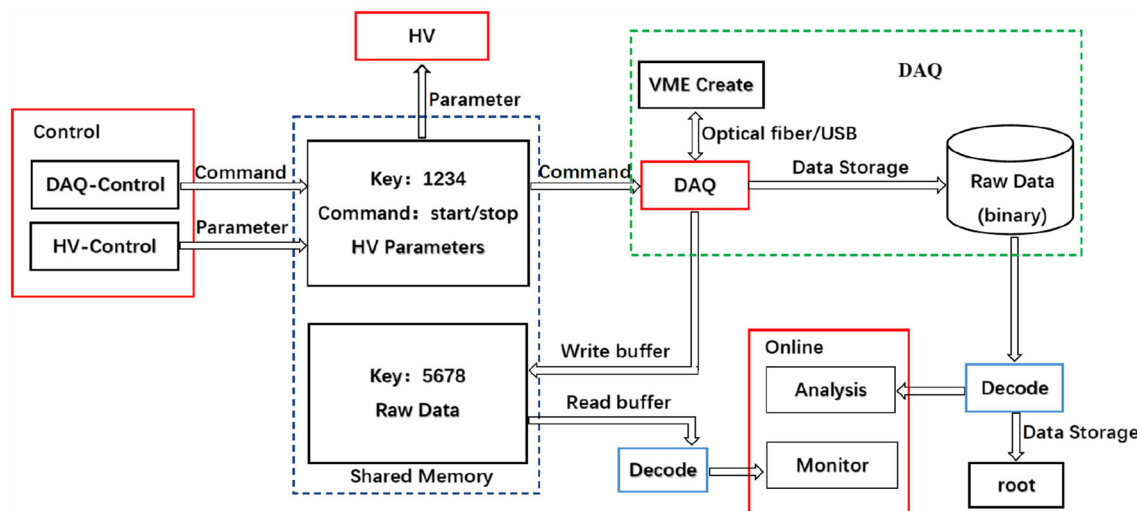

Fig. 2 Frame diagram of software

instructions, and the corresponding feedback parameters. The implementation of HV_Control is based on the shared memory class and HV_class defined in the software. The HV_class calls the CAENHV Wrapper library, which is a software library for power supply control, issued by CAEN to realize the control of DT5533.

The data acquisition module (DAQ_module) receives commands from the Controller_module via shared memory. When the DAQ_module receives the start command, it controls the VME bus to acquire the data. After each data acquisition loop ends, an increasing voltage signal is fed back to the HV_module which waits for the next instruction from the Controller_module. Once the trigger logic triggers a physical event for data acquisition, the events are recorded in the register of the front-end electronics (V785, V775, MADC-32,etc.), and then read by the external first-in first-out (FIFO) memory. Finally, the data in FIFO are transmitted to the PC via optical fiber and stored in the hard disk in binary format for future offline analysis and query. Simultaneously, the raw data will also be transmitted to shared memory for online monitoring through the write buffer. Alternatively, the data can also be acquired by a digitizer [29]. The input pulses, which come from detectors coupled with a charge-sensitive preamplifier (such as HPGe, silicon, etc.) or detectors coupled with PMT, SiPM, etc.,. are digitized into many samples by the flash ADC. Based on the sampling frequency of the digitizer, users can set the number of sampling points according to the width of the waveform by the configuration file. For example, the sampling frequency of DT5720 is 250 MS/s which means sampling a point every 4 ns if a waveform with a width of 1 μs, 250 points were sampled. Each sampled data set can be analyzed to extract the information of time, energy, and so on using the software. Because of the differences in the interface, the base class of the data acquisition modules in the software is divided into two types: the base class of the module with the VME interface and USB interface. The modules with VME_interface, such as ADC (V785, MADC-32, etc.), TDC (V775, MTDC-32, etc.), and QDC (V792, MQDC-32, etc.) are inherited from the base class of the VME interface. The flash ADC contains both modules with a VME interface and a USB interface, which are inherited from two different base classes. Although the flash ADC is divided into two categories, the basic functions are the same. The obtained data are transmitted through the shared memory class, and the parameters passed to the shmget function in the shared memory class are transferred as an array of float type or int type.

The Online_module is mainly composed of two parts: monitoring and analysis. Periodically (every 10 s in the present test system), raw data stored in the front-end electronic registers (e.g., the event number, time stamp, and each channel's energy) can be monitored by online processes through the shared memory mechanism (Online, Fig. 2). The received raw data has a defined data structure, such as the existence of a header(including channel, ID, event count, etc.), datum, and end of event mark. Therefore, to achieve an online monitoring function, it is necessary to call the RawData class (defined in the software) to extract the necessary information from the raw data. In addition to the real-time display of the spectrum of the obtained data, the Online_module can automatically select the analysis algorithm to search for the peak position and set the fitting parameters to fit different spectra according to the radioactive source used in the test. The analysis function of the Online_module first converts the binary data into a ROOT format file after the data acquisition ends, and then analyzes the ROOT file using the corresponding algorithm. During detector unit tests, all data acquisition parameters and analysis processes are saved as a log file for future queries. Furthermore, the analysis results of energy resolution, peak position, and other measurements will also be stored in the disk in txt format.

3.2 Graphical user interface (GUI)

To facilitate user operation, a graphical user interface(GUI) was designed. The GUI is divided into two parts: the main control interface and the online monitor and analysis interface. The GUI was compiled based on ROOT under the Linux system. As shown in Fig. 3, the Controller_module serves as the hub for instruction transfer and parameter adjustment. It is composed of two parts: DAQ_Control and HV_Control, which are associated with the DAQ_module and HV_module, respectively.

The DAQ_Control part of the GUI shown on the left side of Fig. 3a, contains the function of setting the data acquisition parameters. Users can run the start/stop command via the button in the top "control" region. In the middle "setup" region, users can set the file name header and running time of every data acquisition. The high voltage value added to the detector is automatically used as a supplement to complete the file name. All raw data were stored in binary format. The information region shows a simple log of the test system. The HV control part shown on the right side of Fig. 3b, allows users to control the high-voltage channel on/off in the left option box, as well as select the current monitoring range and accuracy. The right part of the HV control shows two high-voltage channel control interfaces. The control interface of each channel displays the default working parameters (modifiable) of DT5533, the monitoring voltage, and current values of the detector. The bottom of each control interface was used to set the voltage range and step interval of the detector test.
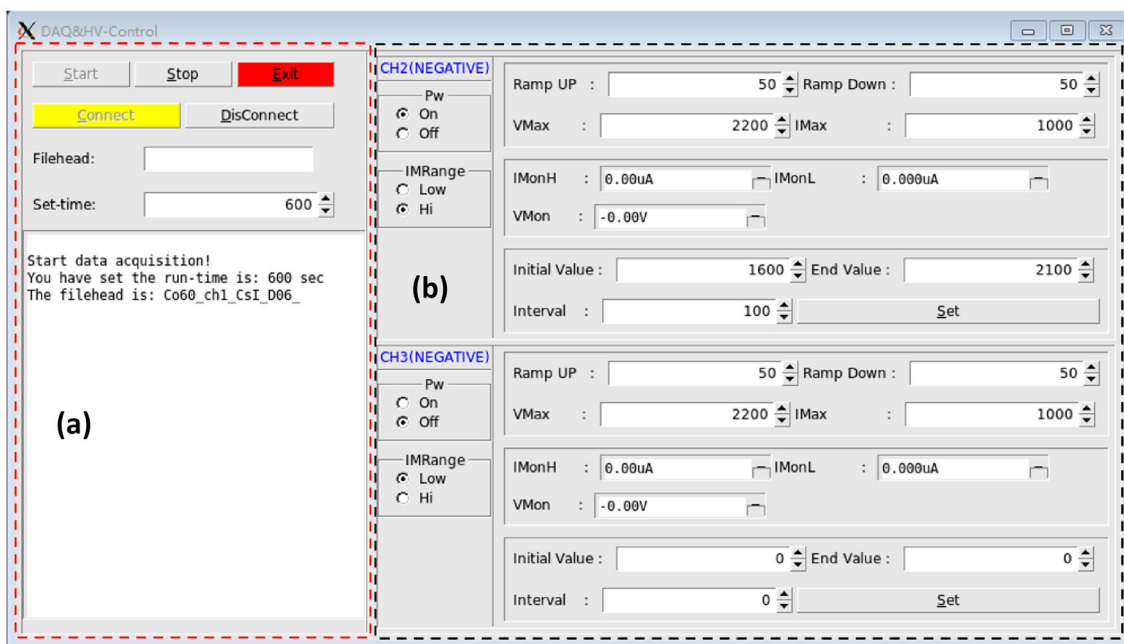
Fig. 3 Interface of Control's GUI:The figure shows the main control interface, through which all the acquisition commands and working parameters can be completed

The main interface of the Online_module contains an online monitor and analysis function. The monitor part reads the raw data from the shared memory in real time. The obtained raw data are decoded first, and then transmitted to the online monitor for spectrum display. The monitored spectrum was updated every ten seconds. Moreover, the monitored channels of each module can be selected in the online GUI. There are also some buttons with specific functions on the online GUI interface. For example, the Online_module can realize an automatic data analysis function through the button "Analysis" on the online GUI. The details of the automatic data analysis function are presented in the next section.

4 System test by CsI detector

The test system was designed for the detector unit test. The feasibility and stability of the system were tested using the CsI detector unit. The CsI detector is one unit of the CsI detector array developed by the Shanghai Institute of Applied Physics, Chinese Academy of Sciences. This array is composed of 42 CsI detector units, which are divided into external and internal layers. The outer layer is composed of 18 units, and the inner layer is divided into two parts; each part consists of 12 units. This array is originally designed to measure the neutron capture (n, γ) cross-section.

4.1 Structure of CsI detector and test

The CsI(TI) crystal of each detector unit of the detector array is a hexagonal prism with a length of 200 mm, and the distance between the opposite sides of the hexagon is 55 mm. The crystal was produced by the Shanghai Institute of Ceramics, Chinese Academy of Sciences, and covered with 1 mm polytetrafluoroethylene(PTFE) and 2 mm thick aluminum as shielding materials. The photomultiplier tube connected to one side of the crystal was R1828-01 (Hamamatsu). The detailed construction of the detector unit can be found in Ref. [19].

To verify the feasibility of the test system, two types of radioactive sources, ^{137}Cs and ^{60}Co, were used to test the performance of the CsI(TI) detector unit. During the test process, the measurement voltage range was set from 1600 to 2100 V, and the measurement interval was set to 100 V. The acquisition time for each condition was set to 10 min. When the Controller_module sends the start instruction to the DAQ_module, it enters the acquisition loop and waits for the feedback signal from the high voltage module (HV_Control). The HV_Control module receives the working parameters from the shared memory. After receiving the corresponding parameters, a high voltage was added to the detector at an initial value of 1600 V. During the voltage raising process, HV_Control feeds back the control status parameters of DT5533 control in real time. Until the voltage-raising operation is completed, DAQ_module starts to control the VME bus to obtain a set of data

under 1600 V. When the running time reaches the set time of 10 min, DAQ_module ends the acquisition loop and returns a raising-voltage signal to HV_Control again. After receiving this signal, HV_Control will raise the voltage to the next target value at a measurement interval of 100 V and feedback the status parameters to control in real time. Then, the Controller_module sends the start command again, and the DAQ_module controls the VME bus to obtain another set of data under 1700 V. The above steps are repeated until the test system obtains the data under 2100 Vat.
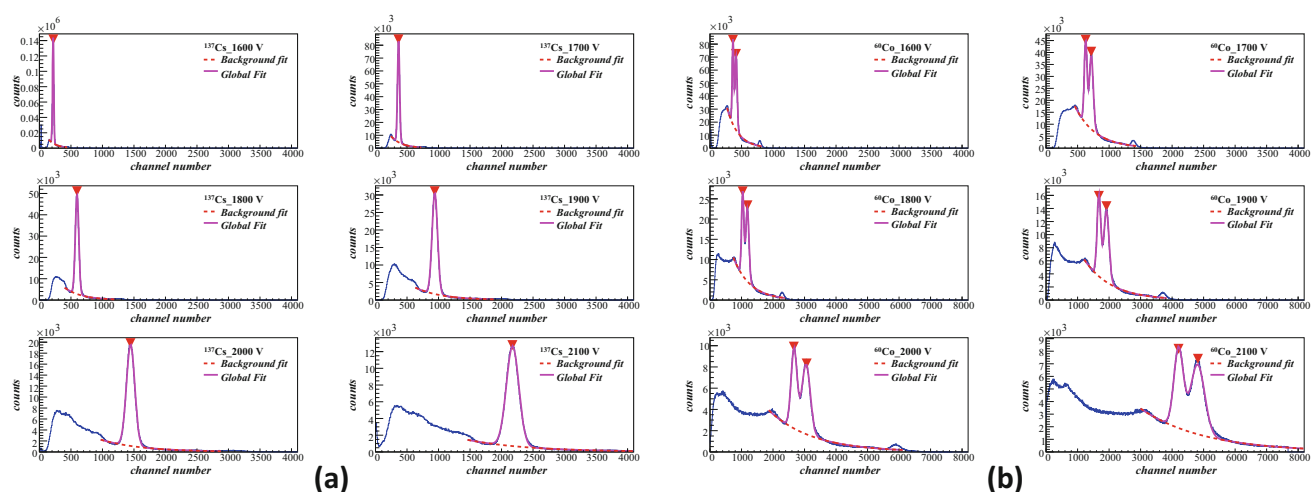
Figure 4 shows the energy spectrum of ^{137}Cs and ^{60}Co obtained by CsI(TI) detector under many different voltages, which are acquired by ADC module V785 or MADC-32. As mentioned in Sect. 3.1, the digitizer, such as DT5720, has been added into the test system. Therefore, the data can also be acquired by digitizer. In this study, the trigger signal of the digitizer is generated by a self-trigger mode. The raw waveform is recorded as 300 samples according to the actual width of waveform output by the CsI detector. Although a single raw data file obtained by DT5720 will take up a large amount of storage space, the advantage is that it retains all the information of the output signal of the detector. Several algorithms have been integrated into the test system to extract energy and time information from sampling data. For example, users can extract the time information via the method of constant fraction discrimination (CFD) or leading-edge discrimination (LED). Since the spectrum obtained by DT5720 is consistent with that obtained by V785 and MADC-32, it is no longer presented in this paper.

4.2 Data online analysis

During the test process of the detector arrays, a great amount of data is acquired resulting in large files. This can result in a time-consuming and tedious offline data analysis. Because the spectrum of radioactive sources used for detector tests is usually known [30], it is possible to program automatic peak searching and spectrum fitting according to different radioactive sources. Users then only need to declare the appropriate radioactive source in the file name, and the Online_module can select the corresponding algorithm to process different raw data.

Typically, the raw data obtained by the analog-to-digital conversion module (ADC, TDC, etc.) are a series of integer values, called channel numbers, which are determined by the resolution of the module. This needs to be converted into the corresponding energy by an energy calibration. Generally, the calibration function of the scintillator detector is nonlinear, and the calibration functions of the silicon detectors and HPGe detectors are linear. Therefore, at least three calibration points are required for the energy calibration. In this study, ^{137}Cs and ^{60}Co sources were used to test the performance of the CsI detector. There are two peaks in the γ-spectrum of ^{60}Co, and the corresponding energies are 1.173 and 1.332 MeV, respectively. There is one peak in the γ-spectrum of ^{137}Cs, and the corresponding energy was 0.662 MeV. It meets the minimum requirement for energy calibration.

For online monitoring and analysis, the raw data must first be decoded, and then the binary file converted into the ROOT file. After this, the Online_module fits and searches for the peak of the spectrum to obtain the channel numbers corresponding to the peaks of the two types of radioactive sources under various voltages, as shown in Fig. 4. Generally, the fitting methods for the ^{137}Cs and ^{60}Co spectra

Fig. 4 Energy spectrum of CsI(TI) detector under ^{137}Cs and ^{60}Co radioactive sources. **a** ^{137}Cs 1600 V-2100 V; **b** ^{60}Co 1600 V-2100 V

are different. Because the energy spectrum of ^{137}Cs has an exponential background and a single Gaussian peak, the fitting algorithm is carried out using a single Gaussian plus an exponential function. However, for the spectrum of ^{60}Co, the fitting algorithm adopts double Gaussian function plus an exponential function because of the existence of double Gaussian peaks and an exponential shape. The corresponding fitting algorithm is integrated into the software. Users only need to declare a radioactive source in the file name.

After fitting the spectrum, the calibration curve of the two sources under different voltages can be obtained, as shown in Fig. 5. The horizontal axis represents the channel number, and the vertical axis represents the energy. When the γ-ray energy was lower than 1.332 MeV, there was a good linear relationship between the energy and channel numbers. As presented above, the calibration curve of scintillator detectors is usually nonlinear. However, because the tested CsI(TI) detector is a large-size detector, high-energy γ photons can deposit all their energy in a CsI(TI) crystal. This makes the calibration curve of the CsI(TI) detectors linear. A detailed discussion can be found in found in [19]. Figure 6 shows one of the results of the analysis. Based on this figure, it can be inferred that a maximum voltage limit can be added to the detectors to prevent the DAQ from exceeding the effective range to excessive working voltage.

To compare the performance of the detector under different voltages, it is necessary to calculate the absolute energy resolution under different conditions. As shown in Figs. 4 and 5, the spectrum fitting and energy calibration
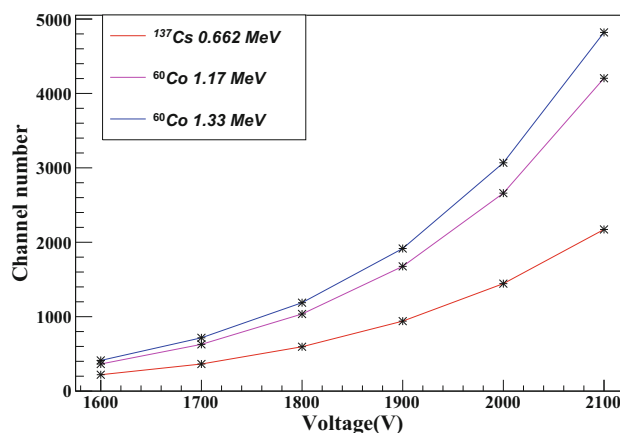

Fig. 6 Curve of peak position versus voltage

under different voltages were completed. Therefore, the FWHM of each peak can be calculated according to the Gaussian fitting parameter using the formula FWHM = 2.355σ, and then it can be converted into energy according to the calibration curve. Figure 7 shows the absolute energy resolution of the CsI(TI) detector under different voltages. It can be inferred from the figure that, when the γ-ray energy is lower than 1.332 MeV, the energy resolution improves with an increase in voltage. In addition to the graphs shown above, other analysis results, such as the energy calibration function, Gaussian fitting parameter σ, absolute energy resolution, and relative energy resolution, will be recorded in the txt file, which is convenient for users to archive and query.

Fig. 5 Energy calibration on different voltage: 1600 V-2100 V
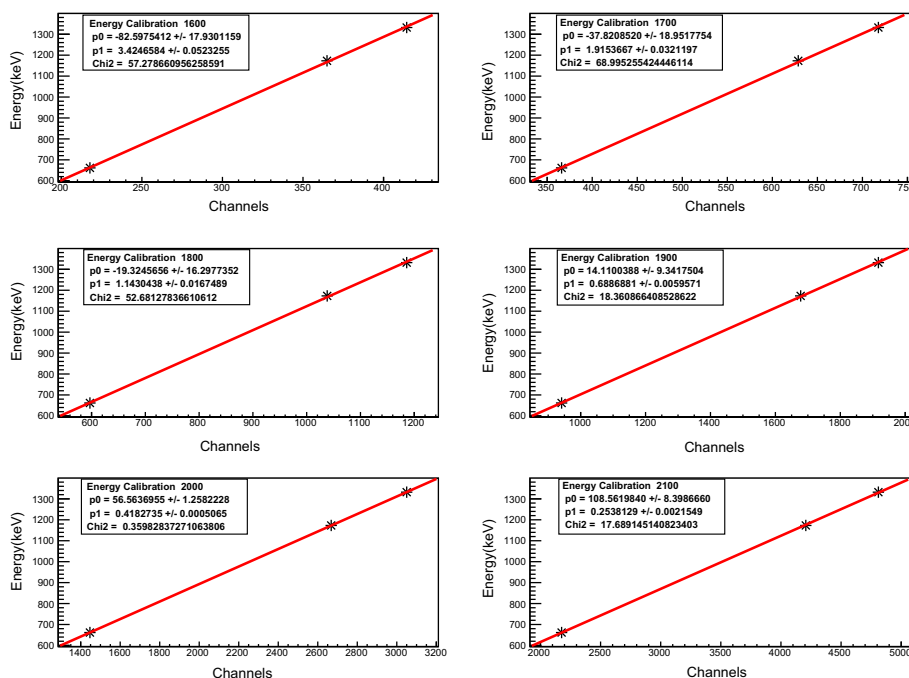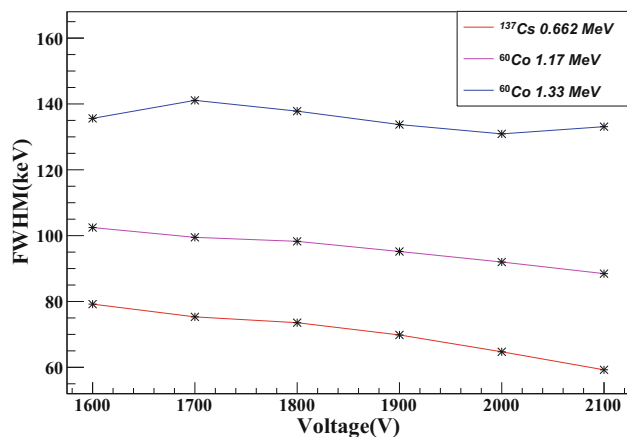
Fig. 7 Absolute energy resolution with a gain of 3.3

5 Summary

This paper reports a ROOT-based detector test system that can automatically adjust the working parameters of the detector and online data analysis. The software of the test system is compiled based on ROOT and runs under the Linux operating system. A user friendly GUI helps users to monitor and control the detector test system easily and efficiently. The test system was successfully applied to the test of a CsI(TI) detector array.

Owing to the modular design of the test system, the system can be easily expanded to match different types of detectors. At present, this study only implements the automatic adjustment of the voltage parameters. However, the test modes supported by the test system can be expanded by adding different function modules. For example, control of the shaping amplifier MSCF-16 can be added to implement the automatic adjustment of gain through the software. A stepping motor slide rail can also be added to the test system to implement a change in the incident position of the radioactive source by controlling the motor slide rail.

In summary, the feasibility and stability of the test system were verified through a CsI(TI) unit test. This shows that the design idea of this test system is feasible and can greatly simplify the test process of the detector unit. Because of the modular architecture of the software, the test system has versatility, scalability, and many useful application prospects.

References

1. S. Akkoyun, A. Algora, B. Alikhani et al., AGATA–advanced GAmma tracking array. Nucl. Instrum. Method Phys. Res. A **668**, 26–58 (2012). https://doi.org/10.1016/j.nima.2011.11.081
2. F. Camera, H. Utsunomiya, V. Varlamov et al., Gamma above the neutron threshold experiments at ELI-NP. Rom. Rep. Phys. **68**, S539–S619 (2016)
3. P. Cardarelli, G. Paternò, G. Di Domenico et al., A gamma beam profile imager for ELI-NP gamma beam system. Nucl. Instrum. Method Phys. Res. A **893**, 109–116 (2018). https://doi.org/10.1016/j.nima.2018.03.023
4. H.C. Scraggs, C.J. Pearson, G. Hackman et al., TIGRESS highly-segmented high-purity germanium clover detector. Nucl. Instrum. Method Phys. Res. A **543**, 431–440 (2005). https://doi.org/10.1016/j.nima.2004.12.012
5. M. Descovich, I.Y. Lee, P. Fallon et al., In-beam measurement of the position resolution of a highly segmented coaxial germanium detector. Nucl. Instrum. Method Phys. Res. A **553**, 535–542 (2005). https://doi.org/10.1016/j.nima.2005.07.016
6. K. Starosta, C. Vaman, D. Miller et al., Digital data acquisition system for experiments with segmented detectors at national superconducting cyclotron laboratory. Nucl. Instrum. Method Phys. Res. A **610**, 700–709 (2012). https://doi.org/10.1016/j.nima.2009.09.016
7. P.-A. Söderström, F. Recchia, J. Nyberg et al., Interaction position resolution simulations and in-beam measurements of the AGATA HPGe detectors. Nucl. Instrum. Method Phys. Res. A **638**, 96–109 (2011). https://doi.org/10.1016/j.nima.2011.02.089
8. T.A. Bredeweg, M.M. Fowler, J.A. Becker et al., Simultaneous measurement of (n, γ) and $(n,$ fission$)$ cross sections with the DANCE 4π BaF2 array. Nucl. Instrum. Method Phys. Res. A **261**, 986–989 (2007). https://doi.org/10.1016/j.nimb.2007.04.226
9. M. Jandel, T.A. Bredeweg, A. Couture et al., GEANT4 simulations of the DANCE array. Nucl. Instrum. Method Phys. Res. B **261**, 1117–1121 (2007). https://doi.org/10.1016/j.nimb.2007.04.252
10. C. Guerrero, U. Abbondanno, G. Aerts et al., The n_TOF total absorption calorimeter for neutron capture measurements at CERN. Nucl. Instrum. Method Phys. Res. A **608**, 424–433 (2009). https://doi.org/10.1016/j.nima.2009.07.025
11. J.F. Perello, S. Almaraz-Calderon, B.W. Asher et al., Characterization of the CATRiNA neutron detector system. Nucl. Instrum. Method Phys. Res. A **930**, 196–202 (2019). https://doi.org/10.1016/j.nima.2019.03.084
12. L. Bardelli, M. Bini, G. Casini et al., Progresses in the pulse shape identification with silicon detectors within the FAZIA Collaboration. Nucl. Instrum. Method Phys. Res. A **654**, 272–278 (2011). https://doi.org/10.1016/j.nima.2011.06.063
13. M. Pfützner, M. Karny, L.V. Grigorenko et al., Radioactive decays at limits of nuclear stability. Rev. Mod. Phys. **84**, 567–619 (2011). https://doi.org/10.1103/RevModPhys.84.567
14. N. Le Neindre, R. Bougault, S. Barlini et al., Comparison of charged particle identification using pulse shape discrimination and ∆E-E methods between front and rear side injection in silicon detectors. Nucl. Instrum. Method Phys. Res. A **701**, 145–152 (2013). https://doi.org/10.1016/j.nima.2012.11.005
15. J.G. Guerra, J.G. Rubiano, G. Winter et al., Modeling of a HPGe well detector using PENELOPE for the calculation of full energy peak efficiencies for environmental samples. Nucl. Instrum. Method Phys. Res. A **908**, 206–214 (2018). https://doi.org/10.1016/j.nima.2018.08.048
16. Z.-Y. Li, Y.-M. Zhang, G.-F. Cao et al., Event vertex and time reconstruction in large-volume liquid scintillator detectors. Nucl.

Sci. Tech. **32**, 49 (2021). https://doi.org/10.1007/s41365-021-00885-z

17. K.L. Giboni, P. Juyal, E. Aprile et al., A LN$_2$-based cooling system for a next-generation liquid xenon dark matter detector. Nucl. Sci. Tech. **31**, 76 (2020). https://doi.org/10.1007/s41365-020-00786-7

18. P. Juyal, K.-L. Giboni, X.-D. Ji et al., On proportional scintillation in very large liquid xenon detectors. Nucl. Sci. Tech. **31**, 93 (2020). https://doi.org/10.1007/s41365-020-00797-4

19. H. Dong, D.-Q. Fang, C. Li, Study on the performance of a large-size CsI detector for high energy γ-rays. Nucl. Sci. Tech. **29**, 7 (2018). https://doi.org/10.1007/s41365-017-0345-1

20. M. Battaglia, D. Bisello, D. Contarato et al., A DAQ system for pixel detectors R&D. Nucl. Instrum. Method Phys. Res. A **611**, 105–110 (2009). https://doi.org/10.1016/j.nima.2009.09.008

21. W.-X. Zhou, Y.-Y. Wang, L.-M. Pan, Design of a NIM-based DAQ system. Nucl. Sci. Tech. **28**, 139 (2017). https://doi.org/10.1007/s41365-017-0296-6

22. H.Y. Wu, Z.H. Li, H. Tan et al., A general-purpose digital data acquisition system (GDDAQ) at Peking University. Nucl. Instrum. Method Phys. Res. A **975**, 164–200 (2020). https://doi.org/10.1016/j.nima.2020.164200

23. A. Balzer, M. Fußling, M. Gajdus et al., A DAQ system for pixel detectors R&D. Nucl. Instrum. Methods A **611**, 105–110 (2009). https://doi.org/10.1016/j.nima.2009.09.008

24. CERN ROOT, https://root.cern.ch/

25. CAEN ADC V785, https://www.caen.it/products/v785/

26. Mesytec MADC-32, http://www.mesytec.com/products/datasheets/MADC-32.pdf

27. Mesytec MSCF-16, http://www.mesytec.com/products/datasheets/MSCF16-F-V.pdf

28. CAEN DT5533, https://www.caen.it/products/dt5533e/

29. CAEN Digitizers, https://www.caen.it/sections/digitizer-families/

30. NuDat2.8, https://www.nndc.bnl.gov/nudat2/